*energies*

*Article*

# A Layered Parallel Equaliser Based on Flyback Transformer Multiplexed for Lithium-Ion Battery System

**Hongrui Liu *, Xiangyang Wei, Junjie Ai and Xudong Yang**

Faculty of Electrical Engineering, Kunming University of Science and Technology, Kunming 650500, China; 20212205024@stu.kust.edu.cn (X.W.); 201910501203@stu.kust.edu.cn (J.A.); 20212205061@stu.kust.edu.cn (X.Y.)
* Correspondence: lhr168@kust.edu.cn; Tel.: +86-156-8710-2699

**Abstract:** An effective equaliser is crucial for eliminating inconsistencies in the connected serial batteries and extending the life of the battery system. The current equalisers generally have the problems of low equalisation efficiency, slow equalisation speed, and complex switching control. A layered parallel equaliser based on a flyback transformer multiplexed for a lithium-ion battery system is proposed. The equaliser employs both hierarchical and parallel equalisation techniques, allowing for simultaneous processing of multiple objectives. This enhances both the efficiency and speed of the equalisation process. The efficiency of equalisation can be further improved by implementing PWM control with deadband complement. Additionally, the flyback transformer serves as an energy storage component for both layers of the equalisation module, resulting in a significant reduction in the size and cost of the equaliser. The circuit topology of the equaliser is presented, and its operational principle, switching control, and equalisation control strategy are analysed in detail. Finally, an experimental platform consisting of six lithium-ion batteries is constructed, and equalisation experiments are conducted to verify the advantages of the proposed equaliser in terms of equalisation speed, efficiency, and cost.

**Keywords:** equaliser; multiplexed flyback transformer; layered parallel equalisation; ithium-ion battery

check for updates

**Citation:** Liu, H.; Wei, X.; Ai, J.; Yang, X. A Layered Parallel Equaliser Based on Flyback Transformer Multiplexed for Lithium-Ion Battery System. *Energies* **2024**, *17*, 754. https://doi.org/10.3390/en17030754

Academic Editor: Carlos Miguel Costa

Received: 16 December 2023
Revised: 18 January 2024
Accepted: 31 January 2024
Published: 5 February 2024



## 1. Introduction

Lithium-ion batteries are commonly used in grid energy storage and electric vehicles due to their high energy density, lack of memory effect, and long cycle life [1]. However, individual lithium-ion batteries have a low nominal voltage that does not meet the requirements for applications such as electric vehicles and energy storage. To achieve the necessary power levels, a large number of individual batteries must be connected in series and parallel [2]. However, lithium-ion batteries inevitably vary in terms of individual capacity and internal resistance during the manufacturing process, leading to inconsistency between batteries. This inconsistency gradually increases during the use cycle, making the battery pack prone to a single overcharge or overdischarge, which seriously affects the overall performance of the battery system. Thus, it is imperative to address the issue of inconsistency among battery system monomers. Battery equalisation technology proves to be an effective solution [3].

There are two main types of equalisation methods: passive equalisation and active equalisation [4,5]. The passive consumes the excess energy through a parallel resistor. Despite its simplicity, the passive equalisation structure results in high energy loss and slow equalisation speed [6].

The active equalisation employs an inductor, capacitor, and transformer as the energy storage elements to transfer energy between batteries. Capacitor-based equalisation is a method of transferring battery energy using capacitance. It controls the on-off of switching devices to transfer energy between adjacent batteries. This method avoids the need for direct electrical connections between batteries [7–9]. Inductor-based equalisation is a method of transferring battery energy using inductance, allowing for highly controllable equalisation currents. However, the process is time-consuming and can negatively impact efficiency [10–14]. LC-based equalisation utilises an inductor (L) and capacitor (C) to form a resonant tank for achieving energy equalisation. However, this method can only work at a specific frequency and duty cycle range, leading to a more complex design and control of LC-based equalisation circuits [15–19].

According to the type of the transformer, transformer-based equalisation can be divided into four types: forward transformer-based equalisation [20], flyback transformer-based equalisation [21,22], forward-flyback transformer-based equalisation [23–25], and multi-winding transformer-based equalisation [16,26–29]. Shang et al. [20] proposed a forward transformer equaliser that uses the voltage difference to automatically transfer energy between batteries. However, as the voltage difference decreases, equalisation becomes more difficult, resulting in poor equalisation results. Guo et al. [21] proposed a flyback transformer equaliser, which has the advantages of easy electrical isolation and simple control. However, the equalisation speed decreases, and the cost and volume increase as the number of series-connected batteries increases. Shang et al. [23] proposed a forward-flyback transformer-based equaliser that reduces the voltage difference between batteries by combining the characteristics of forward and flyback transformers. The equalisation speed is improved because the forward transformer is used before the flyback transformer. However, the equalisation effect of the forward transformer is poor when the voltage difference is small. Liu et al. [26] proposed a multi-winding transformer-based equaliser using forward conversion, which is easy to control, but the equalisation speed is slow, and the equalisation effect is poor when the voltage difference is low.

This paper proposes a layered parallel equaliser based on a flyback transformer multiplexed for a lithium-ion battery system to address the design issues mentioned above.

(1) The equaliser uses a layered equalisation mode to double the input voltage and improve equalisation efficiency. Additionally, the use of complementary PWM control with a dead band reduces switching loss, further improving equalisation efficiency.
(2) The parallel equalisation mode is utilised to enable simultaneous charging or discharging of multiple batteries or battery units, resulting in a significant improvement in equalisation speed.
(3) The equaliser employs flyback transformers as multiplexed energy storage elements, reducing both cost and size. The primary winding of the flyback transformer acts as an inductor in the first-layer equalisation, facilitating energy transfer between the two batteries. In the second-layer equalisation, the flyback transformer functions as an energy storage element, facilitating energy transfer between battery units through an energy transfer unit.
(4) The equaliser has a modular design, allowing for the simple addition of equalisation modules as the number of batteries connected in series increases while maintaining the parameters within the equalisation module.

The paper is structured into six sections. Section 2 provides a detailed explanation of the layered equalisation working principle and MOSFET control. Section 3 introduces the equalisation control strategy. Section 4 presents the experimental platform parameters, procedure, and results. Section 5 presents a comparative analysis of the proposed equaliser with various types of equalisers. Section 6 provides a general description of the main features of the proposed equaliser and identifies areas for improvement. Finally, Section 7 analyses the conclusion.

## 2. Proposed Equaliser

### 2.1. Structure of the Proposed Equaliser

The architecture of the proposed equaliser is illustrated in Figure 1 and consists of two equalisation modules: the first-layer equalisation module (FMi) and the second-layer equalisation module (SMi). The battery pack is divided into a single battery (Bi) and a battery unit (BUi) according to the equalisation process. The first-layer equalisation module primarily achieves energy equalisation between two single batteries within the battery unit. The second-layer equalisation module aims to achieve energy balance between the battery units. Once the first-layer equalisation is complete, the second-layer equalisation begins.

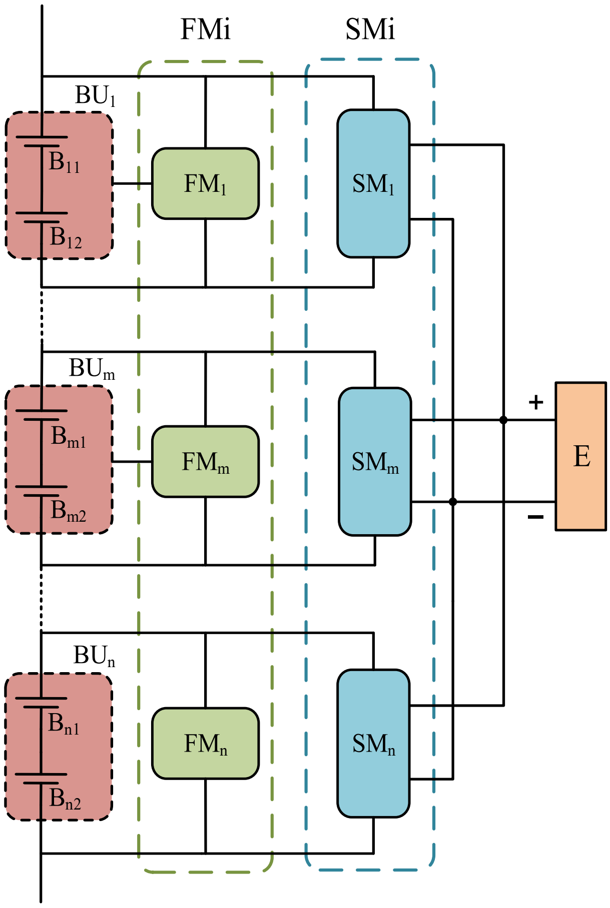


**Figure 1.** The architecture of the proposed equaliser.

The circuit topology of the proposed equaliser is shown in Figure 2, which consists of a battery system of n single batteries connected in series, n/2 flyback transformers, 3n MOSFETs, and an energy transfer unit E. Six MOSFET switches with anti-parallel diodes (Mi1 to Mi6) and a flyback transformer Ti form an equalisation module. Each battery unit BUi consists of two single batteries, which correspond to an equalisation module. The energy transit unit E is composed of two single batteries connected in series.

### *2.2. Operating Principle of the Proposed Equaliser*

#### 2.2.1. Operating Principle of the First-Layer Equalisation

To address the energy equalisation issue between two single batteries in the battery unit, the primary winding Li1 of the transformer is utilised as the energy storage component. The first-layer equalisation works in DCM mode in order to avoid the situation of magnetic saturation of the inductor. The corresponding switches adopt complementary PWM with a headband in order to further improve equalisation efficiency.

SOCBij represents the state of charge of the battery Bij. Taking batteries B11 and B12 as an example, assuming SOCB11 > SOCB12. Figure 3 shows the key waveforms of the first-layer equalisation. The first-layer equalisation stage can be divided into four steps.

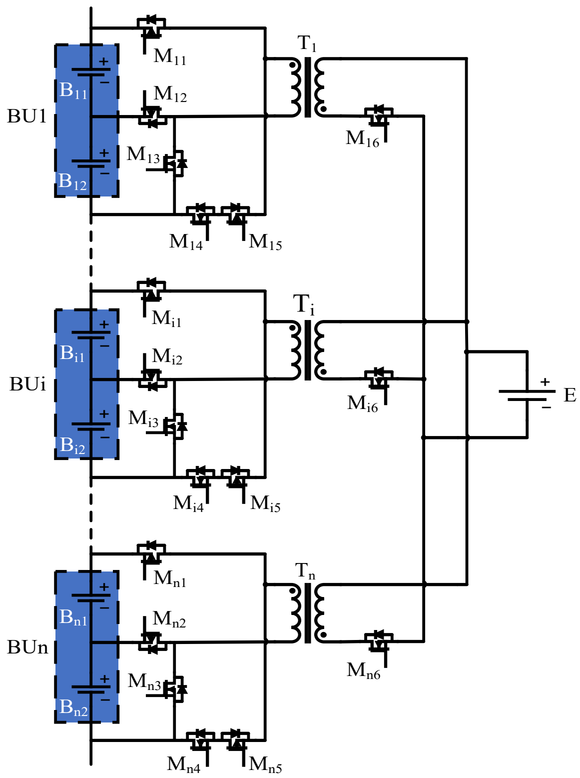


**Figure 2.** The circuit topology of the proposed equaliser.

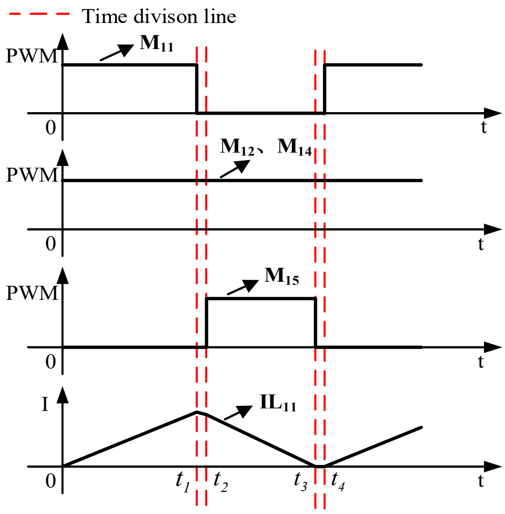


**Figure 3.** The key waveforms in the first-layer equalisation.

State I [$0-t_1$]: As shown in Figure 4a, M11 is turned on, M12 and M14 and M14 are stayed on, and the energy of B11 is transferred to the primary winding L11 of transformer T1. In this state, the current of the inductor L11 can be expressed as

$$i_{L11} = \frac{V_{B11} - 2V_{mos}}{L_{11}} t \tag{1}$$

where $i_{L11}$ and $L_{11}$ are the current and the inductance of L11, respectively. $V_{B11}$ is the input voltage, $V_{mos}$ is the conduction voltage drop of MOSFET.

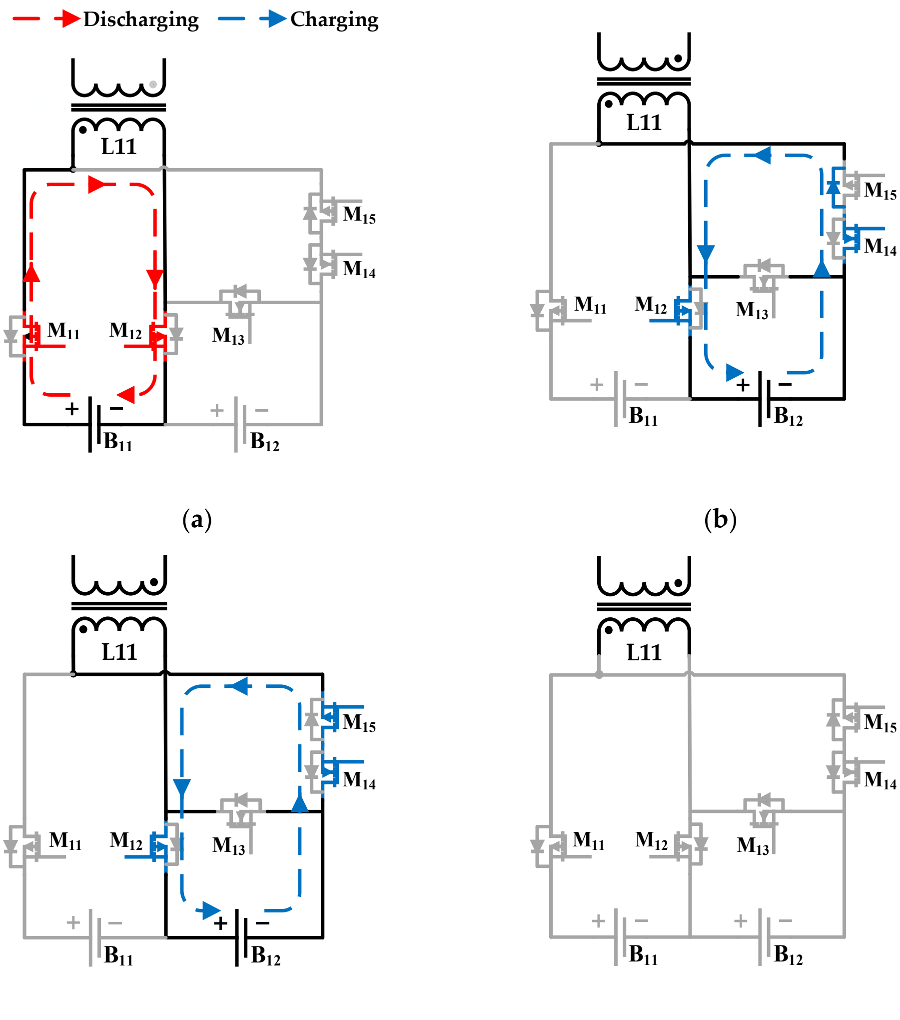


**Figure 4.** Operational states of the first−layer equalisation. (**a**) State I. (**b**) State II. (**c**) State III. (**d**) State IV.

State II $[t_1-t_2]$: As shown in Figure 4b, M11 is turned off, and then the energy in L11 flows to the battery B12 through the reverse parallel diode of M15. In this state, the current of L11 can be expressed as

$$i_{L11} = i_{L11}(t_1) - \frac{V_{out}+2V_{mos} + V_D}{L_{11}}(t - t_1) \quad (2)$$

where $t_1$ is the turn-on time of M11, $t_1$ is the output voltage, $V_D$ is the forward voltage of the reverse parallel diodes of MOSFETs.

State III $[t_2-t_3]$: As shown in Figure 4c, M15 is turned on, and then the energy of L11 is transferred to battery B12. In this state, the current of L11 can be expressed as

$$i_{L11} = i_{L11}(t_2) - \frac{V_{out}+3V_{mos}}{L_{11}}(t - t_2) \quad (3)$$

State IV $[t_3-t_4]$: As shown in Figure 4d, M11, M13, M15 are turned off, and the current of L11 is zero. This indicates that the first-layer equalisation has been completed.

Considering the conduction losses of diodes and MOSFETs, the efficiency of the first-layer equalisation is:

$$\eta_1 = 1 - \frac{2\int_0^{t_1} R_{ds} {i_{L11}}^2 dt + \int_{t_1}^{t_2} i_{B12}(V_D + 2R_{ds} i_{L11})dt + 3\int_{t_2}^{t_3} R_{ds} {i_{L11}}^2 dt}{\int_0^{t_1} V_{B11} i_{L11} dt} \tag{4}$$

where $R_{ds}$ is the on-resistance of MOSFETs, $i_{L11}$ is the RMS current of L11.

### 2.2.2. Operating Principle of the Second-Layer Equalisation

The second-layer equalisation utilises the flyback transformer to transfer energy between different battery units via the energy transfer unit E. This process ultimately achieves energy equalisation among all battery units within the entire battery system. The equalisation process can be carried out simultaneously on multiple battery units during discharging or charging. High-energy battery units transfer energy to the energy transfer unit E during discharging, and the energy of E is transferred to low-energy battery units simultaneously. Additionally, the equalisation speed increases with the number of parallel equalisation targets.

To determine which battery unit is discharged or charged in the second-layer equalisation, it is necessary to compare the average value of all battery units, SOCBUi, with the average value of the SOC of the battery pack, SOCavg. As the first-layer equalisation is complete, the SOC values of B11 and B12 are equal, the SOC values of B21 and B22 are equal, and the SOC values of B31 and B32 are equal, respectively: SOCBU1 = SOCB11 = SOCB12, SOCBU2 = SOCB21 = SOCB22, and SOCBU3 = SOCB31 = SOCB32. For instance, let us consider the battery units BU1, BU2, and BU3. It is assumed that SOCBU1 > SOCBU2 > SOCavg > SOCBU3. The equalisation process can be divided into two states.

State I: As shown in Figure 5a, M11 and M21 are turned on, while M13 and M23 remain on. L11 absorbs and stores the energy released by battery units BU1 and BU2. The current on L11 can be expressed as

$$i_{L11} = \frac{V_{BU1} - 2V_{mos}}{L_{11}} t \tag{5}$$

where $V_{BU1}$ is the voltage of BU1 and $L_{11}$ is the inductance of the primary winding of T1.

The current $i_{L21}$ on the primary winding L21 of T2 is as stated above.

When M11 and M21 are turned off, the energy induced by the secondary winding flows to E through the anti-parallel diodes of switches M16 and M26. At this stage, the current on the secondary winding L12 of T1 can be expressed as

$$i_E = \frac{V_{BU1} - 2V_{mos}}{L_{11}} DT + \frac{V_{BU2} - 2V_{mos}}{L_{21}} DT - \frac{V_{out} + V_D}{L_{12}}(t - DT) - \frac{V_{out} + V_D}{L_{22}}(t - DT) \tag{6}$$

where $L_{12}$ and $L_{22}$ are the inductance of the secondary winding of T1 and T2, respectively. $V_{out}$ is the out voltage, D is the duty cycle of MOSFETs, T is the cycle-time.

State II: As shown in Figure 5b, M36 is turned on, and then E releases energy to the secondary winding L32 of T3. The current of E can be expressed as

$$i_E = \frac{V_E - V_{mos}}{L_{32}} t \tag{7}$$

where $V_E$ is the voltage of E.

When M36 is turned off, M13 remained on. The energy stored in L31 is transferred to the battery unit BU3 through the anti-parallel diode of M31. The current of E can be expressed as

$$i_{L31} = \frac{V_E - V_{mos}}{L_{32}} DT - \frac{V_{out} + V_{mos} + V_D}{L_{31}}(t - DT) \tag{8}$$

Using the BU1 discharging as an example and considering the conduction losses of diodes and MOSFETs, the efficiency $\eta_2$ of the second-layer equalisation is:

$$\eta_2 = 1 - \frac{2\int_0^{DT} R_{ds} {i_{L11}}^2 dt + \int_{DT}^{(D+\alpha)T} V_D i_{L12} dt}{\int_0^{DT} V_{BU1} i_{L11} dt} \tag{9}$$

where $\alpha$ is the duty cycle required to release energy from the secondary winding L12 of T1.

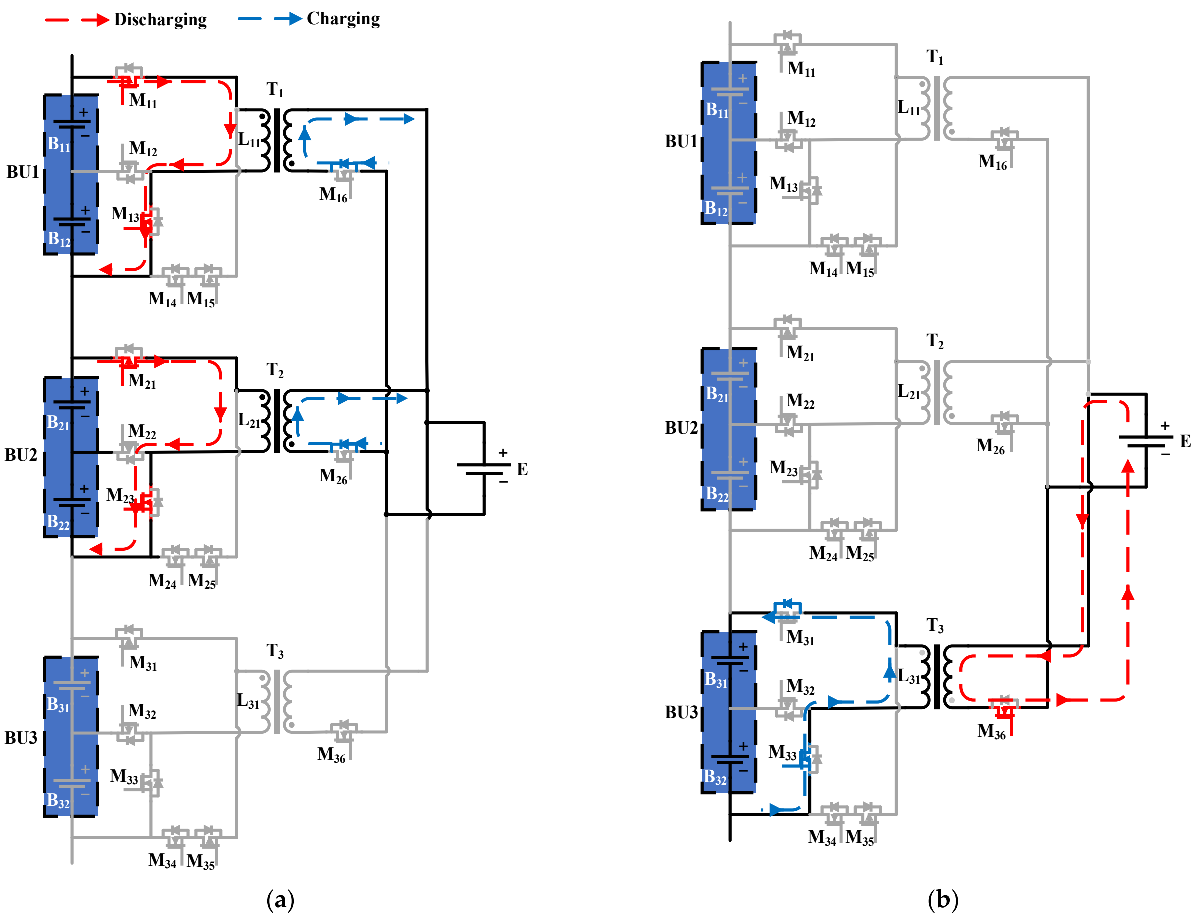


**Figure 5.** Operational states of the second-layer equalisation. (**a**) State I. (**b**) State II.

## 3. Equalisation Strategy Design

Figure 6 shows the equalisation control strategy of a layered parallel equaliser based on a flyback transformer multiplexed for a lithium-ion battery system. The control procedure for MOSFET equalisation is divided into two sequential layers. Before beginning the first-layer equalisation, it is necessary to estimate the quiescent state of charge (SOC) for all batteries.

The first-layer equalisation occurs when the difference in SOC between two batteries within the battery units exceeds the threshold value $\varepsilon$. The battery with the higher SOC value discharges, while the battery with the lower SOC value charges. The second-layer equalisation can only occur after all battery units have undergone internal equalisation. If any battery units remain unequalised, the first-layer equalisation will be repeated. The second-layer equalisation begins when the average SOC value SOCBUi of each battery unit differs from the average SOC value SOCavg of the battery pack by $\varepsilon$. Battery units larger than SOCavg discharge to the energy transfer unit E, while battery units smaller than SOCavg absorb energy from E. When the difference between the average SOC value SOCBUi of all the battery units and the average SOC value SOCavg of the battery pack is within the threshold value $\varepsilon$, the equalisation process ends.

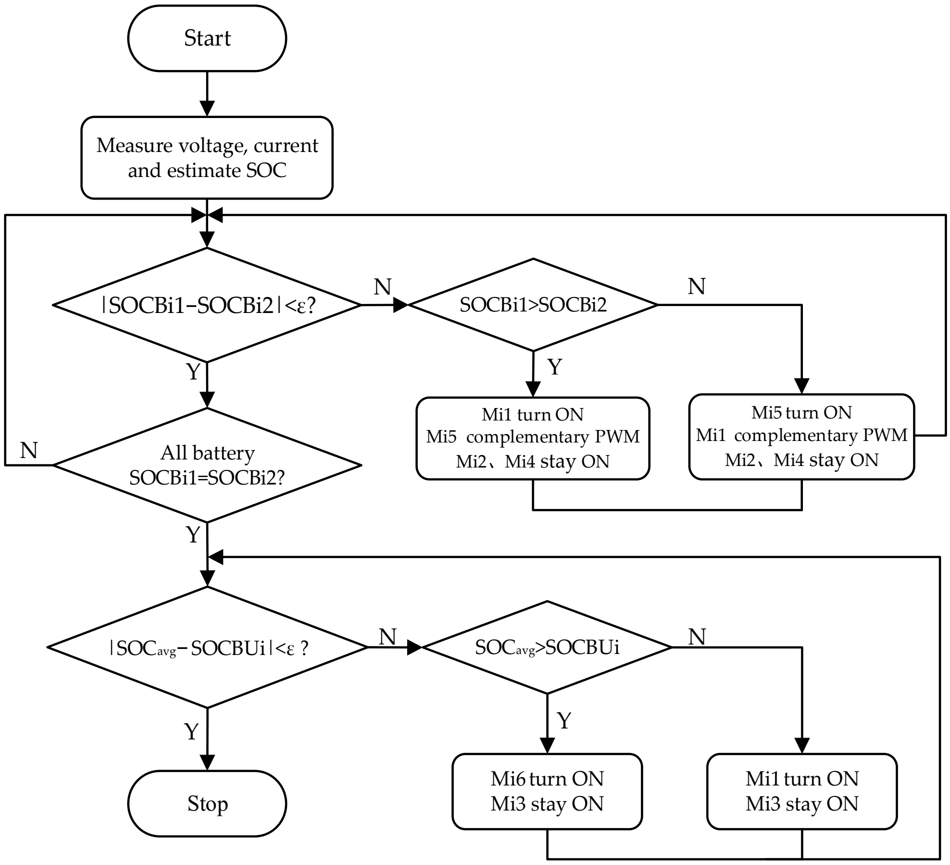


**Figure 6.** The equalisation strategy of the proposed equaliser.

## 4. Equalisation Experiment

### *4.1. Experimental Platform and Parameters*

To demonstrate the effectiveness of this equaliser, an equalisation experimental platform consisting of six series-connected batteries was built, as shown in Figure 7. The rated voltage of the battery is 3.6 V, and the rated capacity is 2600 mAh. The equalisation experimental platform mainly consists of Labview, Battery String, Energy Transfer Battery, Measurement Module, Isolated Drive Supplies, Equaliser, Controller, DC Power Source and Oscilloscope. Table 1 shows the important parameters of the equalisation circuit.

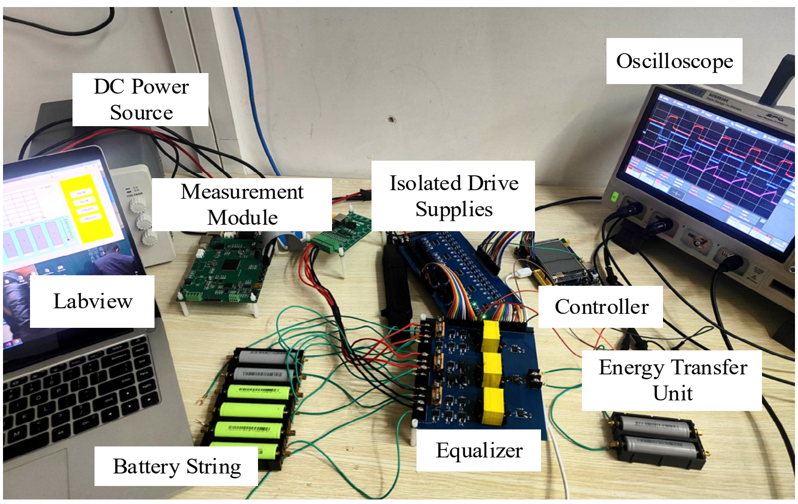


**Figure 7.** Experiment platform.

**Table 1.** Experimental parameters.

| Parameters | | Value |
|---|---|---|
| Battery | Model<br>Nominal capacity<br>Nominal voltage | LS18650-10A<br>2600 mAh<br>3.6 V |
| MOSFET | $M_{ij}$ | TTD85N03AT<br>($V_{DS}$ = 10 V, $I_D$ = 85 A,<br>$R_{DS}$ = 4.5 mΩ) |
| Transformer | $N_1$:$N_2$<br>$L_m$<br>$L_k$ | 1:1<br>21 μH<br>0.1 μH |
| | Equalisation start threshold ($\varepsilon$) | 0.1% |
| | Switching frequency of the first-layer equalisation ($f_1$) | 50 kHz |
| | Switching frequency of the second-layer equalisation ($f_2$) | 50 kHz |

The parameters for the equalisation circuit above are also applicable to a battery system composed of 2n (where n = 1, 2. . ., ∞) batteries connected in series.

### *4.2. The First-Layer Equalisation Experiment*

Table 2 displays the initial SOC values of each battery. During the first-layer equalisation process, batteries B11, B21, and B31 are discharged simultaneously, while batteries B12, B22, and B32 are charged simultaneously. This allows for internal equalisation of the three battery units to occur simultaneously.

**Table 2.** Initial SOC value of each single battery.

| Battery Number | SOC (%) | Voltage (V) | Battery Number | SOC (%) | Voltage (V) |
|---|---|---|---|---|---|
| B11 | 82.39 | 3.898 | B22 | 67.34 | 3.891 |
| B12 | 76.88 | 3.896 | B31 | 62.75 | 3.888 |
| B21 | 72.68 | 3.894 | B32 | 57.28 | 3.884 |

Figure 8a shows the waveform of the current in the battery unit BU2 when the battery B21 is discharged and the waveforms of the complementary PWM driving signals of the switches M11 and M14 in the course of the experiment. Figure 8b shows the waveform of the current in the battery unit BU2 when the battery B22 is charged and the waveforms of the complementary PWM driving signals of the switches M11 and M14 in the course of the experiment. The equalisation current is about 2 A, the duty cycle for M11 is about 31%, the conduction duty cycle of M14 is about 67%, and the driving signals for both switches have a dead time of about 2%.

### *4.3. The Second-Layer Equalisation Experiment*

The second-layer equalisation experiment of the battery system contains three battery units, where the battery unit whose average SOC value $SOCBUi_{avg}$ is higher than the battery system average SOC value SOCavg releases energy, and the battery unit whose average SOC value SOCBUiavg is lower than the battery system average SOC value SOCavg absorbs energy.

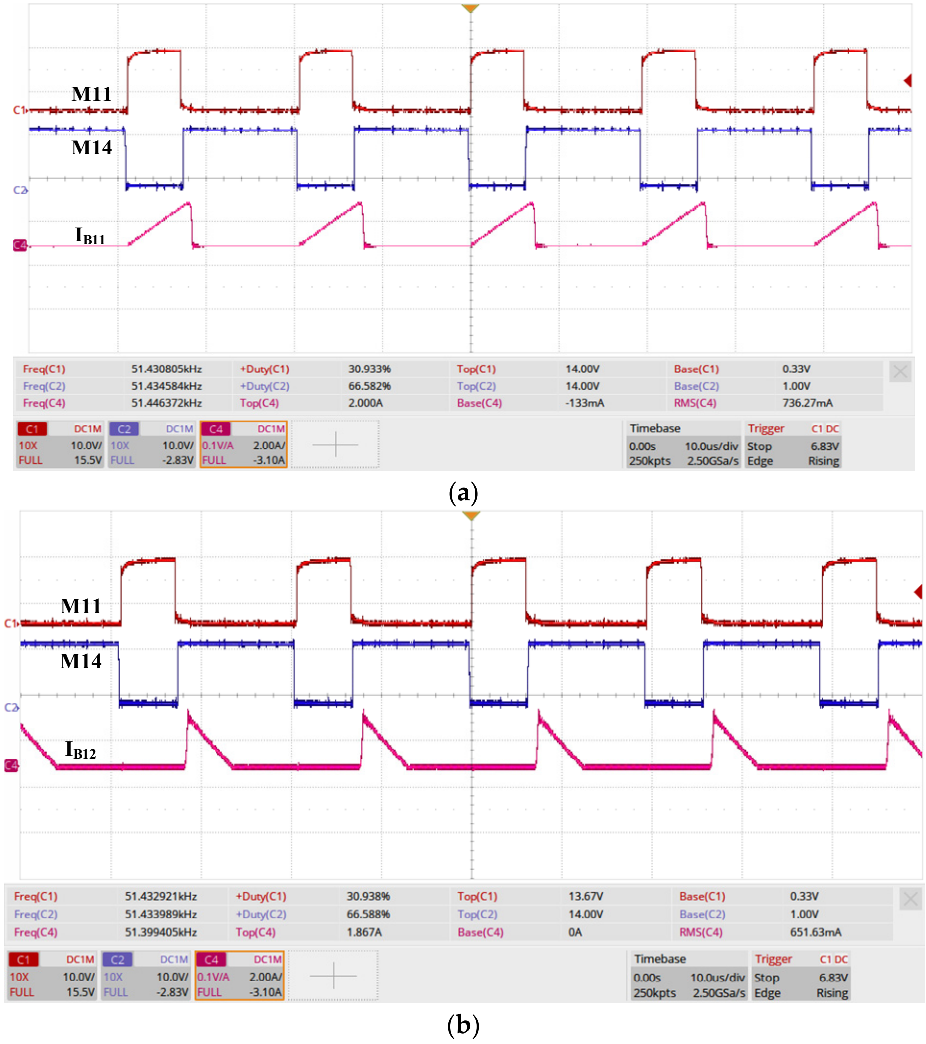


**Figure 8.** Experimental waveforms of the first-layer equalisation. (**a**) PWM signal waveforms of M11, M14 and discharging current waveform of B11. (**b**) PWM signal waveforms of M11, M14 and charging current waveform of B12.

Figure 9a shows the discharging current waveform of battery unit BU1 and the driving signal waveform of switching device M11 intercepted during the experiment. Figure 9b shows the charge current waveform of the energy transit battery E and the driving signal waveform of the switching device M11. The equalisation current is 2.467 A, and the conduction duty cycle of M11 is about 35%.

### *4.4. Equalisation experiment results*

Figure 10 shows that the battery with a high SOC value in each battery unit releases energy, the battery with a low SOC value absorbs energy, and finally the SOC values between the two batteries reach the same. The equalisation times for the three battery units are 20 min, 21 min and 21 min, respectively, so the time required for the first layer of equalisation is 21 min. After equalisation, the SOCs of the three battery units are 79.44%, 70.11% and 59.89%, respectively.

Figure 10 also shows that the battery unit with a high SOC value in the battery system releases energy, and the battery unit with a low SOC value absorbs the energy. This process continues until the SOC values of all three battery units in the system are equalised. The second-layer equalisation process takes 77 min. Following equalisation, the SOC values of all three battery units are 69.85%.

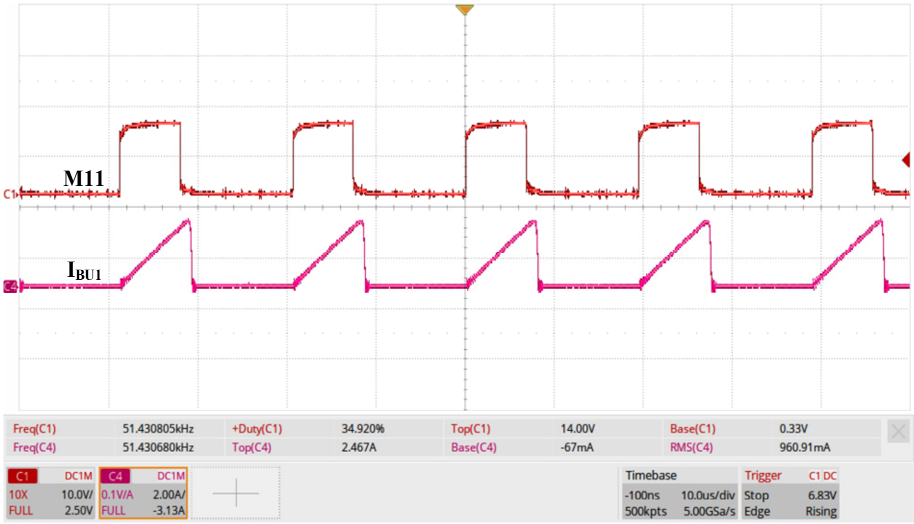


(**a**)

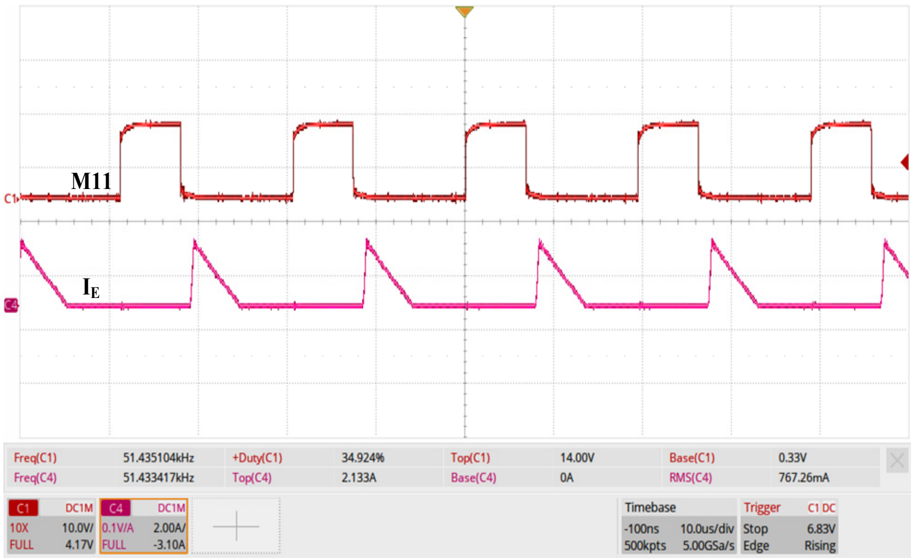


(**b**)

**Figure 9.** Experimental waveforms of the second-layer equalisation. (**a**) PWM signal waveforms of and discharge current waveform of BU1. (**b**) PWM signal waveforms of M11 and charge current waveform of E.

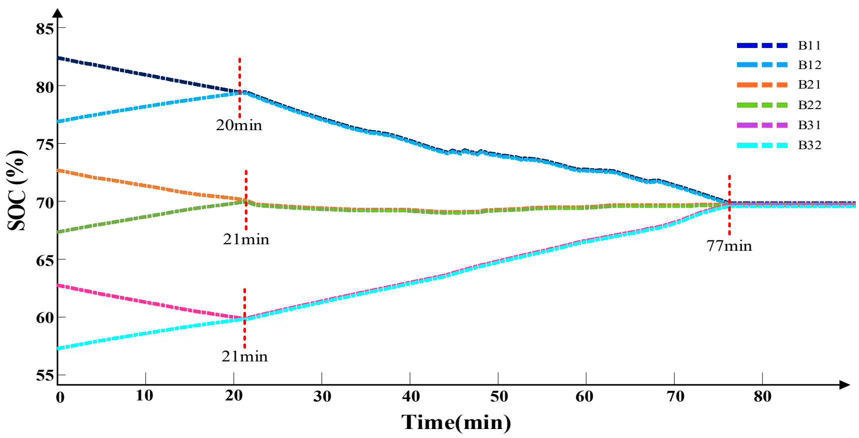


**Figure 10.** SOC curves of the battery string during the equalisation experiment.

## 5. Analysis of Experimental Results

### *5.1. Calculation of Equalisation Efficiency*

#### 5.1.1. Equalisation Efficiency of the First-Layer Equalisation

The first-layer equalisation utilises PWM with deadband complementary to operate the MOSFETs, resulting in reduced switching losses and improved equalisation efficiency. For instance, when considering batteries B11 and B12, the equalisation efficiency of the first-layer can be calculated using Equation (4) according to the relevant parameters and graphs from the equalisation experiment. The calculation process is shown as follows:

$$\begin{aligned}\eta_1 &= 1-\frac{2\int_0^{0.31T}4.5\times10^{-3}\times0.736^2dt+\int_{0.31T}^{0.32T}0.651\times\left(0.6+2\times4.5\times10^{-3}\times0.651\right)dt+3\int_{0.32T}^{0.65T}4.5\times10^{-3}\times0.651^2dt}{\int_0^{0.31T}3.898\times0.736dt} \\ &\approx 98.8\%\end{aligned} \tag{10}$$

#### 5.1.2. Equalisation Efficiency of the Second-Layer Equalisation

The second-layer equalisation process doubles the voltage of the battery unit by using it as the equalisation object. For instance, in the case of battery unit BU2, the equalisation efficiency of the second layer is calculated using Equation (9) and the relevant parameters and graphs from the equalisation experiment. The calculation process is shown as:

$$\eta_2 = 1-\frac{2\int_0^{0.35T}4.5\times10^{-3}\times0.961^2dt+\int_{0.35T}^{0.67T}0.6\times0.767dt}{\int_0^{0.35T}(3.894+3.891)\times0.961}\approx 94.3\% \tag{11}$$

### *5.2. Comparison with Other Methods*

To demonstrate the advantages of the proposed layered parallel equaliser based on a flyback transformer multiplexed for a lithium-ion battery system. Table 3 lists the equalisers that are compared with different types of equalisers in terms of the number of devices and equaliser performance. The number of devices included in the equaliser determines the size and cost of the equaliser, which is mainly compared to the number of MOSFETs (M), diodes (D), inductors (L), capacitors (C), and transformers (T) included in different types of equalisers. This paper classifies the comparison of equalisers into three categories: low (L), medium (M), and high (H), based on their cost, complexity, speed, efficiency, and size.

**Table 3.** Comparison of existing equalisers.

| Equalisers | Components | | | | | Equalisation Performance | | | | |
|---|---|---|---|---|---|---|---|---|---|---|
| | M | D | L | C | T | Cost | Efficiency | Speed | Complexity | Volume |
| [9] | 2N | 0 | 0 | N − 1 | 0 | L | 93.1% | L | M | L |
| [10] | 4N + 2 | 0 | N − 1 | 0 | 0 | H | 80% | M | H | M |
| [15] | 4N | 0 | N | N | 0 | H | 95.2% | L | H | L |
| [16] | 2N | 0 | 2N | N | N | H | 92% | M | H | H |
| [18] | 4N + 1 | 0 | 1 | 1 | 0 | M | 96.05% | L | H | L |
| [19] | N/2 | 0 | N/2 | 0 | 0 | M | / | M | H | M |
| [20] | N | 1 | N/2 | 0 | N/4 | L | 95.6% | M | L | H |
| [22] | 2N + 6 | 0 | 1 | 0 | 1 | M | 80.4% | L | M | L |
| [25] | 5/4N | 0 | 5/4N | 0 | N/4 | M | 93.15% | M | L | M |
| [28] | 2N | 0 | N | 0 | 1 | M | 70.14% | L | M | L |
| Proposed equaliser | 3N | 0 | 0 | 0 | N/2 | M | 98.8%/94.3% | H | M | M |

The proposed equaliser uses a flyback transformer as an equalisation element. To provide a more intuitive comparison, it will be compared with a design based on transformer equalisation. In [16], half-bridge LC transformers are used as an equalisation topology. This topology uses more transformers and inductors, which are larger in size. Due to the fact that equalisation circuit is more intricate, the MOSFET control method is complex. The equaliser described in [22] only requires a flyback transformer, and the volume is small. Equalisation can only be conducted sequentially between batteries, and the equalisation speed is slow. The equalisation path contains more MOSFETs for energy flow, resulting in high switching losses and low equalisation efficiency. The topology in [25] employs multi-winding transformers as the equalisation element, resulting in faster equalisation with fewer MOSFETs and higher efficiency. However, it is unable to selectively charge during the charging process. In [28], the topology also employs multi-winding transformers as equalisation elements. However, as the number of batteries in series increases, the transformer has too many windings, resulting in poor equalisation efficiency.

Table 3 compares the proposed equaliser with various types of equalisers. It is evident that the proposed equaliser outperforms other equalisers in terms of efficiency and speed. Additionally, the proposed equaliser requires fewer components, resulting in a smaller size and lower cost.

## 6. Discussion

This paper proposes a layered parallel equaliser based on flyback transformer multiplexing for a lithium-ion battery system that has higher equalisation efficiency, faster equalisation speed, and greater scalability than other transformer-based equalisation designs. The equaliser employs layered and parallel equalisation to improve efficiency and speed. Additionally, the size of the equaliser is reduced by using a flyback transformer as a two-layer energy storage element. The efficiency of the equaliser is further improved by the short energy path and the small number of MOSFETs passing through the equalisation loop. The equaliser has a modular design and is highly scalable, with component parameters remaining constant as the number of series-connected batteries increases, making it suitable for large-scale energy storage battery systems. However, there are some areas for improvement in this proposed equaliser. For instance, the suggested equaliser uses a greater number of MOSFETs. By decreasing the number of MOSFETs, the cost of the equaliser can be further reduced. Additionally, MOSFET losses can be minimised through the implementation of resonant soft-switching techniques. It is anticipated that this can be improved in future research.

## 7. Conclusions

Aiming at the problems of slow equalisation speed, low equalisation efficiency and weak modularity in the large-scale energy storage lithium-ion battery system, this paper proposes a layered parallel equaliser based on a flyback transformer multiplexed for a lithium-ion battery system. The equaliser has the following characteristics:

1. High equalisation efficiency. The equaliser adopts a layered equalisation strategy. The first-layer equalisation targets a single battery and utilises a Buck-Boost circuit and complementary PWM driving method to prevent energy reflux. This approach results in low equalisation loss and high efficiency. The second-layer equalisation focuses on the battery unit and doubles the voltage to improve equalisation efficiency. This is achieved through a multi-winding transformer equalisation circuit. The first and second layer equalisation experiments resulted in an efficiency of 98.8% and 94.3%, respectively.
2. Fast equalisation speed. The multi-objective parallel equalisation method is utilised by the equaliser. The first-layer equalisation ensures that equalisation within each battery cell does not interfere with each other. The more parallel equalisation targets there are, the faster the entire battery system can be equalised. The second-layer equalisation module uses flyback transformers to parallel discharge or charge multiple battery units. It also enables simultaneous charging and discharging of multiple units, significantly increasing the speed of equalisation.
3. Strong modularity. With an increase in the number of series-connected batteries, the hardware parameters of the equaliser remain unchanged. It is only necessary to adjust the number of corresponding equalisation modules according to needs, which

greatly improves the equaliser's scalability. The equaliser is suitable for a large-scale lithium-ion battery energy storage system.

**Author Contributions:** H.L. proposed the equalisation ideal, X.W. designed the equaliser. X.W., X.Y. and J.A. conceived the research methods and control strategies. X.W. and J.A. designed and performed the experiments. X.W. completed the initial draft, H.L. completed the proofreading of the manuscript. All authors have read and agreed to the published version of the manuscript.

**Funding:** This work is supported by the National Natural Science Foundation of China (51967009).

**Data Availability Statement:** Data are contained within the article.

**Conflicts of Interest:** The authors declare no conflict of interest.

## References

1. Deng, J.; Bae, C.; Marcicki, J.; Masias, A.; Miller, T. Safety modelling and testing of lithium-ion batteries in electrified vehicles. *Nat. Energy* **2018**, *3*, 261–266. [CrossRef]
2. Hannan, M.A.; Lipu, M.S.H.; Hussain, A.; Mohamed, A. A review of lithium-ion battery state of charge estimation and management system in electric vehicle applications: Challenges and recommendations (Review). *Renew. Sustain. Energy Rev.* **2017**, *78*, 834–854. [CrossRef]
3. Zhao, Z.Y.; Hu, H.T.; He, Z.Y.; Iu, H.H.C.; Davari, P.; Blaabjerg, F. Power Electronics-Based Safety Enhancement Technologies for Lithium-Ion Batteries: An Overview from Battery Management Perspective. *IEEE Trans. Power Electron.* **2023**, *38*, 8922–8955. [CrossRef]
4. Ghaeminezhad, N.; Ouyang, Q.; Hu, X.S.; Xu, G.T.; Wang, Z.S. Active Cell Equalization Topologies Analysis for Battery Systems: A Systematic Review. *IEEE Trans. Power Electron.* **2021**, *36*, 9119–9135. [CrossRef]
5. Izadi, Y.; Beiranvand, R. A Comprehensive Review of Battery and Supercapacitor Cells Voltage-Equalizer Circuits. *IEEE Trans. Power Electron.* **2023**, *38*, 15671–15692. [CrossRef]
6. Shang, Y.L.; Zhu, C.; Fu, Y.H.; Mi, C.C. An Integrated Heater Equalizer for Lithium-Ion Batteries of Electric Vehicles. *IEEE Trans. Ind. Electron.* **2019**, *66*, 4398–4405. [CrossRef]
7. Ye, Y.M.; Cheng, K.W.E.; Fong, Y.C.; Xue, X.D.; Lin, J.J. Topology, Modeling, and Design of Switched-Capacitor-Based Cell Balancing Systems and Their Balancing Exploration. *IEEE Trans. Power Electron.* **2017**, *32*, 4444–4454. [CrossRef]
8. Lee, S.; Noh, G.; Ha, J.I. Reconfigurable Power Circuits to Series or Parallel for Energy-Balanced Multicell Battery Pack. *IEEE Trans. Ind. Electron.* **2023**, *70*, 3641–3651. [CrossRef]
9. Shang, Y.L.; Cui, N.X.; Duan, B.; Zhang, C.H. Analysis and Optimization of Star-Structured Switched-Capacitor Equalizers for Series-Connected Battery Strings. *IEEE Trans. Power Electron.* **2018**, *33*, 9631–9646. [CrossRef]
10. Wang, S.; Yang, S.; Yang, W.; Wang, Y. A New Kind of Balancing Circuit with Multiple Equalization Modes for Serially Connected Battery Pack. *IEEE Trans. Ind. Electron.* **2021**, *68*, 2142–2150. [CrossRef]
11. Ding, X.F.; Zhang, D.H.; Cheng, J.W.; Wang, B.B.; Chai, Y.M.; Zhao, Z.H.; Xiong, R.; Luk, P.C.K. A Novel Active Equalization Topology for Series-Connected Lithium-ion Battery Systems. *IEEE Trans. Ind. Appl.* **2020**, *56*, 6892–6903. [CrossRef]
12. Manjunath, K.; Kalpana, R.; Singh, B.; Kiran, R. A Two-Stage Module Based Cell-to-Cell Active Balancing Circuit for Series Connected Lithium-Ion Battery Packs. *IEEE Trans. Energy Convers.* **2023**, *38*, 2282–2297. [CrossRef]
13. Wang, L.J.; Ke, J.Y.; Zhan, M.; Tian, A.N.; Jiang, J.C. Efficient and Fast Active Equalization Method for Retired Battery Pack Using Wide Voltage Range Bidirectional Converter and DBSCAN Clustering Algorithm. *IEEE Trans. Power Electron.* **2022**, *37*, 13824–13833.
14. Peng, F.; Wang, H.; Yu, L. Analysis and Design Considerations of Efficiency Enhanced Hierarchical Battery Equalizer Based on Bipolar CCM Buck–Boost Units. *IEEE Trans. Ind. Appl.* **2019**, *55*, 4053–4063. [CrossRef]
15. Liu, L.; Mai, R.; Xu, B.; Sun, W.; Zhou, W.; He, Z. Design of Parallel Resonant Switched-Capacitor Equalizer for Series-Connected Battery Strings. *IEEE Trans. Power Electron.* **2021**, *36*, 9160–9169. [CrossRef]
16. Liu, F.; Zou, R.; Liu, Y. An Any-Cell-to-Any-Cell Battery Equalizer Based on Half-Bridge LC Converter. *IEEE Trans. Power Electron.* **2023**, *38*, 4218–4223. [CrossRef]
17. Wei, Z.; Wang, H.; Lu, Y.; Shu, D.; Ning, G.; Fu, M. Bidirectional Constant Current String-to-Cell Battery Equalizer Based on L2C3 Resonant Topology. *IEEE Trans. Power Electron.* **2022**, *38*, 666–677. [CrossRef]
18. Noh, G.; Lee, J.; Ha, J.-I. Design and Analysis of Single-Inductor Power Converter for Both Battery Balancing and Voltage Regulation. *IEEE Trans. Ind. Electron.* **2022**, *69*, 2874–2884. [CrossRef]
19. Reema, N.; Jagadanand, G.; Sasidharan, N.; Shreelakshmi, M.P. An Enhanced Coupled Inductor Based Voltage Equalizer for Matrix Connected Ultracapacitor Bank. *IEEE Trans. Transp. Electrif.* **2023**, *9*, 3328–3337. [CrossRef]
20. Shang, Y.; Cui, N.; Duan, B.; Zhang, C. A Global Modular Equalizer Based on Forward Conversion for Series-Connected Battery Strings. *IEEE J. Emerg. Sel. Top. Power Electron.* **2018**, *6*, 1456–1469. [CrossRef]
21. Guo, X.; Geng, J.; Liu, Z.; Xu, X.; Cao, W. A Flyback Converter-Based Hybrid Balancing Method for Series-Connected Battery System in Electric Vehicles. *IEEE Trans. Veh. Technol.* **2021**, *70*, 6626–6635. [CrossRef]

22. Lee, K.M.; Lee, S.W.; Choi, Y.G.; Kang, B. Active Balancing of Li-Ion Battery Cells Using Transformer as Energy Carrier. *IEEE Trans. Ind. Electron.* **2017**, *64*, 1251–1257. [CrossRef]
23. Shang, Y.; Xia, B.; Zhang, C.; Cui, N.; Yang, J.; Mi, C.C. An Automatic Equalizer Based on Forward–Flyback Converter for Series-Connected Battery Strings. *IEEE Trans. Ind. Electron.* **2017**, *64*, 5380–5391. [CrossRef]
24. Narayanan, R.; Gangadharan, J.; Sasidharan, N.; Meleetil, P.S. A Novel Modularization Method for Voltage Equalization of Ultracapacitor Bank Using Coupled Inductor. *IEEE Trans. Ind. Electron.* **2024**, *71*, 3548–3558. [CrossRef]
25. Wang, S.; Wang, Y.; Chen, G.; Wei, D.; Shang, Y. An Efficient and Compact Equalizer Based on Forward-Flyback Conversion for Large-Scale Energy Storage Systems. *IEEE Trans. Transp. Electrif.* **2023**, *early accessed*. [CrossRef]
26. Liu, L.; Xu, B.; Yan, Z.; Zhou, W.; Li, Y.; Mai, R.; He, Z. A Low-Cost Multiwinding Transformer Balancing Topology for Retired Series-Connected Battery String. *IEEE Trans. Power Electron.* **2021**, *36*, 4931–4936. [CrossRef]
27. Fan, S.; Duan, J.; Sun, L.; Zhang, K. A Fast Modularized Multiwinding Transformer Balancing Topology for Series-Connected Super Capacitors. *IEEE Trans. Power Electron.* **2019**, *34*, 3255–3268. [CrossRef]
28. Chen, Y.; Liu, X.; Cui, Y.; Zou, J.; Yang, S. A MultiWinding Transformer Cell-to-Cell Active Equalization Method for Lithium-Ion Batteries with Reduced Number of Driving Circuits. *IEEE Trans. Power Electron.* **2016**, *31*, 4916–4929.
29. Nie, J.; Fu, R.; Cai, C.; Ma, J.; Shu, Z.; Ma, L. A High Efficiency Battery Equalizing Circuit Based on Half Bridge Topology with Multiport Transformer. *IEEE Trans. Ind. Electron.* **2024**, *71*, 2522–2532. [CrossRef]